ELSEVIER

International Journal of Mass Spectrometry 185/186/187 (1999) 913–923

International Journal of Mass Spectrometry

Binding energies of chromium cations with fluorobenzenes from radiative association kinetics

Victor Ryzhov, Chia-Ning Yang, Stephen J. Klippenstein*, Robert C. Dunbar*

Department of Chemistry, Case Western Reserve University, Cleveland, OH 44106, USA

Received 26 August 1998; accepted 16 November 1998

Abstract

The addition of electron-withdrawing substituents to an aromatic ring is expected to weaken the cation/π-face binding via electron withdrawal from the π system. In order to characterize this effect quantitatively in a well behaved model system, rates of radiative association of Cr^+ with the complete set of fluorobenzenes, $C_6H_{6-n}F_n$, where $n = 0 - 6$, were measured in the Fourier transform ion cyclotron resonance mass spectrometer. Radiative association rates are very sensitive to the ion-neutral bonding strength, and well established kinetic modeling methods permit the extraction of binding energy values from association observations. Modeling was based on variational transition state theory, using Becke-3 Lee-Yang-Parr (B3LYP) density functional theory-calculated vibrational frequencies and infrared emission intensities of the ion-neutral complexes. The resulting "experimental" binding energies were compared with B3LYP density functional theory calculations for these systems. The calculations indicate that an in-plane fluorine bridging binding site is favored for those neutrals having two adjacent fluorine substituents, while otherwise π-facial binding is favored. The "experimental" binding energies and the B3LYP density functional theory-calculated binding energies of the most favorable sites agree within about 10%. The π-face binding strength decreases by roughly 5 kcal mol^{-1} with each added fluorine substituent on the ring. (Int J Mass Spectrom 185/186/187 (1999) 913–923) © 1999 Elsevier Science B.V.

Keywords: Binding energy; Radiative association; Fourier-transform ion cyclotron resonance; Fluorobenzenes; Chromium ions

1. Introduction

The interaction of metal ions with the π faces of aromatic molecules constitutes a central concern of organometallic chemistry. Contemporary experimental techniques and computational capabilities allow such interactions to be explored with increasing quantitative confidence. The bound-metal environment varies with substituents on the ring, with fluorine substitution giving among the most dramatic effects owing to its strong electron-withdrawing power. Increasing fluorine substitution is expected to make the electrostatic potential above the ring more positive, leading to a decrease in binding energy of cationic partners. An example of this fluorine effect was shown by Schwarz' group in the comparison of Au^+ binding to benzene (70 kcal mol^{-1}) and hexafluorobenzene (31 kcal mol^{-1}) [1].

The present study set out to explore these fluorine-substituent effects quantitatively by both experimental and theoretical determination of the binding energies of Cr^+ to the complete set of fluorobenzenes. In the

* Corresponding authors.

Dedicated to Professor Michael T. Bowers on the occasion of his 60th birthday.

PII S1387-3806(98)14271-9

course of the theoretical part of the work, it became clear that fluorine binding sites existed with comparable stability to the expected ring π binding site, and it was necessary to characterize these sites as well.

Chromium ion is an attractive metal ion for this study. In comparison with nontransition metal ions, for instance Na^+, *d*-orbital participation greatly enhances the binding energy (40 kcal mol^{-1} for Cr(benzene)$^+$ [2,3] versus 28 kcal mol^{-1} for Na(benzene)$^+$ [4]), which enlarges the range of binding energies available in a comparative study like this. In comparison with other transition metal ions, the d^5 half-filled *d*-orbital shell makes the ion relatively unreactive, simplifying the chemistry. The theoretical modeling is also simplified and made more certain by the need to consider only one electronic state. Moreover, the binding energy of Cr^+ to the benzene π face happens to fall in a convenient energy range for study by the radiative association (RA) kinetics approach used in the experimental part of this study.

The present paper presents the experimental results, the assignment of the binding energies via kinetic modeling, and the interpretation of the binding energy trends along the series. A companion paper [5] presents the details of the quantum chemistry theoretical studies and their application to the kinetic modeling, giving fuller consideration to the complex geometries and the various binding sites available to the metal ion.

The rates of radiative association are extremely sensitive to the binding energy of the complex. This makes it possible to determine the binding energy of complexes by measuring and analyzing the radiative association kinetics. Modeling of radiative association processes based on variational transition state theory (VTST) and employing quantum chemical estimates of IR frequencies and intensities has yielded reasonable binding energy values for several systems and has given us some confidence in the validity and utility of this approach [3,6–8]. Here we used it to extract the binding energy values of Cr^+ with the complete set of fluorobenzenes. Two characteristics of these systems make them very attractive for radiative association studies. First, they cover a very wide range of binding energies and second, they all have the same number of degrees of freedom which enables us to separate the binding energy dependence of radiative association rates from size effects.

Another attractive feature of these systems is the fact that the polarizabilities are similar (9.58–9.86 $Å^3$) and are close to the polarizability of benzene (10.39 $Å^3$). This implies similar contributions of the ion-induced-dipole interaction to the overall binding, simplifying the interpretation of the binding energy trends.

It is also interesting to compare these "experimental" binding energy values with the corresponding B3LYP density functional theory quantum chemical estimates. Such comparisons are important since the calculations give valuable information on the geometry of complexes, which is not available from our experiments.

It was suggested [2,9] that the transition metal ion binding to benzene is primarily electrostatic, although it is clear that covalent components of the bonding are not insignificant for transition metal ion binding to π faces. Electrostatic arguments can bring insight to comparing metal-ion affinities of various binding sites [10–14]. The electrostatic potential of benzene has a negative value above the ring [13], providing the good π binding site responsible for the many known metal-ion/benzene complexes. However, the electrostatic potential of hexafluorobenzene actually has a positive value above the ring [13], thus making π binding unfavorable for cations. (As a matter of fact, π binding of an anion, Au^-, to C_6F_6 has recently been observed [15].) The increasingly unfavorable electrostatic environment for cations above the ring with fluorine substitution not only leads to the expectation of decreasing binding energies, but also makes it likely that other non-π cation binding sites will become important. Exploring these questions calls for a combination of experimental and theoretical approaches.

2. Experimental

Experiments were performed on a modified Nicolet FT-2000 ICR mass spectrometer. A schematic of the instrument is shown in Fig. 1. The vacuum

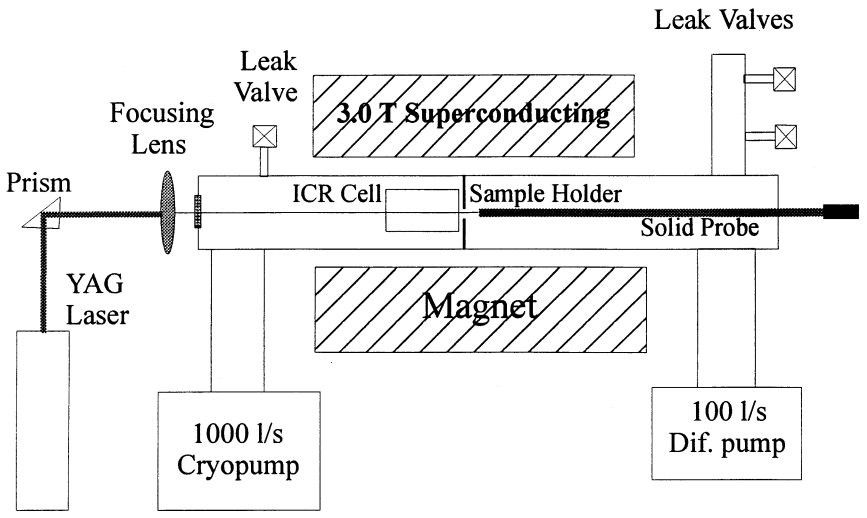

Fig. 1. Schematic of the Nicolet FT-2000 ICR mass spectrometer.

chamber is located inside the 15 cm bore of a 3.0 T superconducting magnet (Oxford). There is a partition with a 3 mm hole in the middle of the vacuum system (conductance limit) dividing the system in two parts. The left part containing a $5 \times 5 \times 10$ cm elongated ICR cell is called the analyzer side. It is pumped by a 1000 l/s Cryo Torr 8 cryopump (CTI Cryogenics) and has a base pressure of 5×10^{-10} Torr. The right part (source side) can contain a second ICR cell which was dismounted for convenience. It is pumped by a 100 l/s diffusion pump (Alcatel) backed by a direct drive mechanical pump giving the base pressure of 1×10^{-8} Torr. Pressure on each side is measured by nude ionization gauge tubes located well outside the magnet and operated by a Granville-Phillips 330 ion gauge controller.

Neutrals were introduced into the cell through leak valves (Varian). The pressure of the neutrals varied from 5×10^{-9} to 5×10^{-7} Torr. Cr^+ ions were formed by laser desorption-ionization by focusing a pulsed 532 nm YAG laser beam on the stainless steel solid probe tip located behind the cell near the hole in the trapping plate. (There is an optical window on the analyzer side of the vacuum system allowing a laser beam to pass through the cell and on the sample holder. In addition, there are 3 mm holes in the trapping plates). Inlet and solid probe pumping is done by a 60 l/s diffusion pump (Alcatel) backed by a direct drive mechanical pump.

After ion formation all Fe^+ ions and Cr^+ isotopes except $^{52}Cr^+$ were removed from the cell by a series of single mass ejection pulses. Then a thermalization period allowing at least 10 ion-neutral collisions was provided. After that the unwanted ionic species were removed by a series of ejection pulses and Cr^+ ions were allowed to react for a time which ranged from 200 ms to 200 s, following which the extent of association was measured as a function of the reaction time.

Data processing and instrument control are done

by an IonSpec data system operated with Omega 5.20 software.

The ion gauge pressure readings were calibrated by fast proton transfer reactions from CH_5^+ ions to benzene, assuming the collisional rate for this reaction. Using this calibration, the rate of radiative association of Cr^+ ions with benzene was measured to be 2.3×10^{-11} cm^3 s^{-1}, in acceptable agreement with the 1.8×10^{-11} cm^3 s^{-1} measured previously [3] on the other instrument in our laboratory. Because substantial effort was devoted to the pressure calibration on the latter instrument, the similar value of the rate constant obtained here with the Nicolet FTICR gives us additional confidence in the pressure calibration.

Benzene and all fluorobenzenes were purchased from Aldrich Chemical Company (Milwaukee, WI) and used without further purification other than repeated freeze-pump-thaw cycles.

3. Computation and modeling details

All geometry optimizations and IR frequencies and intensities calculations were done using density functional theory (DFT) with the 6-31G* basis set on C, H, and F and the 6-311+G* basis set on Cr^+. The Becke-3 Lee-Yang-Parr (B3LYP) hybrid functional was adopted. All binding energies were calculated at the same computational level, with zero-point energy corrections from full vibrational frequency sets, and with basis set superposition error (BSSE) corrections following the geometry-relaxed scheme of Xantheas [16]. All calculations were done using GAUSSIAN 94 software [17]. Full computational details and results are available in the companion paper [5].

An association reaction is normally analyzed in terms of the mechanism (1):

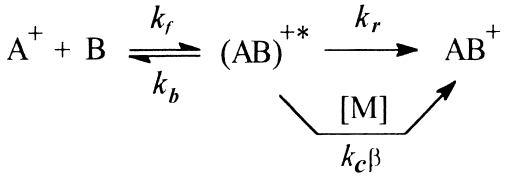

(1)

where k_f is the bimolecular rate constant for collisional complex formation, k_b is the unimolecular redissociation rate constant, k_r is the unimolecular rate constant for IR photon emission from the energized complex, and $k_c\beta$ is the bimolecular rate constant for collisional stabilization of $(AB)^{+}$* by collision with neutral M. $(AB)^{+}$* is the metastable collision complex. In the low-pressure regime the kinetics are bimolecular at any given pressure [18], with apparent bimolecular rate constant k_2.

At low pressures where three-body collisional stabilization of the complex is negligible, the association becomes purely radiative; the overall bimolecular rate constant can be called k_{ra}, and is given by:

$$k_2(\text{low pressure}) = k_{ra} = k_f k_r /(k_b + k_r) \qquad (2)$$

Deriving thermochemical conclusions from radiative association kinetics data relies on kinetic modeling. The most complete approach to this task has used a theoretical framework based on variational transition-state theory (VTST) [7], combined with quantum chemical calculations of the required geometries, IR frequencies and intensities of the metastable complex. This approach has given excellent results in terms of calculating and combining the microscopic rate constants in Eq. (1) to predict accurate association kinetics [3,6,8,19].

Because it is central to the analysis, a brief review of this methodology is provided here. The present VTST methodology employs an approximate separation of modes into the vibrational modes of the fragments, termed the conserved modes, and the remaining rotational and orbital modes of the fragments, termed the transitional modes. The conserved mode contribution to the transition state number of available states is evaluated via a direct sum over the harmonic oscillator vibrational levels. That for the transitional modes is instead evaluated via Monte Carlo based integration of classical phase space integrals employing the long-range representation for the ion-molecule potential. The transition state number of states correlates with the minimum in the number of

available states as a function of the separation between the fragments. This transition state number of states is then employed in consistent evaluations of the formation rate constants k_f and the dissociation rate constants k_b. The partition functions for the complex and the free fragments assume rigid-rotor harmonic-oscillator energetics.

The implementation of the ion-induced dipole potential for the long range potential provides the standard Langevin result for k_f. Many of the fluorobenzenes have a non-zero permanent dipole moment which leads to a measurably increased transition state partition function and correspondingly larger k_f and k_b values. The ion-dipole potential is explicitly included in the present VTST evaluations leading to dipole corrected results which, for related systems, have been found [20] to be in good agreement with trajectory results of Su and Chesnavich [21]. In some instances the dipole moments are not well known and scaled B3LYP-DFT calculated dipole moments are instead employed. A scale factor of 0.8 is applied to these computed dipole moments on the basis of comparison between the known and calculated fluorobenzene and 1,3-difluorobenzene dipole moments.

The radiative relaxation of the complex is assumed to be dominated by IR emission. The radiative rate constants, k_r, were evaluated from the B3LYP-DFT quantum chemical estimates for the intensities of the IR fundamental absorption bands.

The VariFlex software package [22], which was employed here, implements these theoretical estimates for k_f, k_b, and k_r in the modeling of the rate constant k_{ra} for the overall radiative association kinetics. Fitting the calculated k_{ra}, as a function of the binding energy between the ion A^+ and the neutral B, to the experimental value of k_{ra} gives the "experimental" value for the binding energy. The rotational constants, vibrational frequencies, and IR radiative intensities, required for this modeling, are each obtained from the B3LYP-DFT calculations, because they are generally not available from experiment. Table 1 collects a number of the molecular parameters used in this study.

Table 1
Molecular parameters of the reactant molecules used in the kinetic modeling

Neutral	α (Å^3)	μ_D (Debye)	k_f[a]
Benzene	10.39[b]	0	13.5
Fluorobenzene	9.86[b]	1.60[d]	18.6
1,2-Difluorobenzene	9.80[b]	2.8[e]	25.7
1,3-Difluorobenzene	9.80[c]	1.58[d]	17.9
1,4-Difluorobenzene	9.80[c]	0	12.2
1,2,3-Trifluorobenzene	9.74[c]	3.09[e]	26.9
1,2,4-Trifluorobenzene	9.74[c]	1.53[e]	17.2
1,3,5-Trifluorobenzene	9.74[b]	0	11.9
1,2,3,4-Tetrafluorobenzene	9.69[c]	2.60[e]	23.4
1,2,3,5-Tetrafluorobenzene	9.69[c]	1.48[e]	16.7
1,2,4,5-Tetrafluorobenzene	9.69[b]	0	11.7
Pentafluorobenzene	9.63[b]	1.47[e]	16.3
Hexafluorobenzene	9.58[b]	0	11.3

[a] Rate constants in units of 10^{-10} cm^3 mol^{-1} s^{-1}.
[b] [23].
[c] All isomers are assumed to have same polarizability.
[d] [24].
[e] Scaled B3LYP-DFT calculations (see text).

4. Results and discussion

4.1. Experimental results

All systems studied here showed simple association behavior (forming CrL^+) followed by sequential CrL_2^+ formation, with no significant competing reaction processes. The possible addition of a third ligand to give CrL_3^+ was not tested except for the benzene and fluorobenzene cases, for which this process was not observed. Rates of association were measured at different pressures of the neutrals. No pressure dependence was observed up to 3×10^{-7} Torr for the reactions of Cr^+ with benzene, fluorobenzene, difluorobenzenes, and trifluorobenzenes. This fact means that under the experimental conditions the association reactions were purely radiative. It was not possible to study the pressure dependence for association of Cr^+ with tetrafluorobenzenes, pentafluorobenzene and hexafluorobenzene. We assumed that association in these systems was also governed by a radiative mechanism.

An illustrative spectrum of Cr^+ reacting with 1,2,3-trifluorobenzene is shown in Fig. 2. Under these

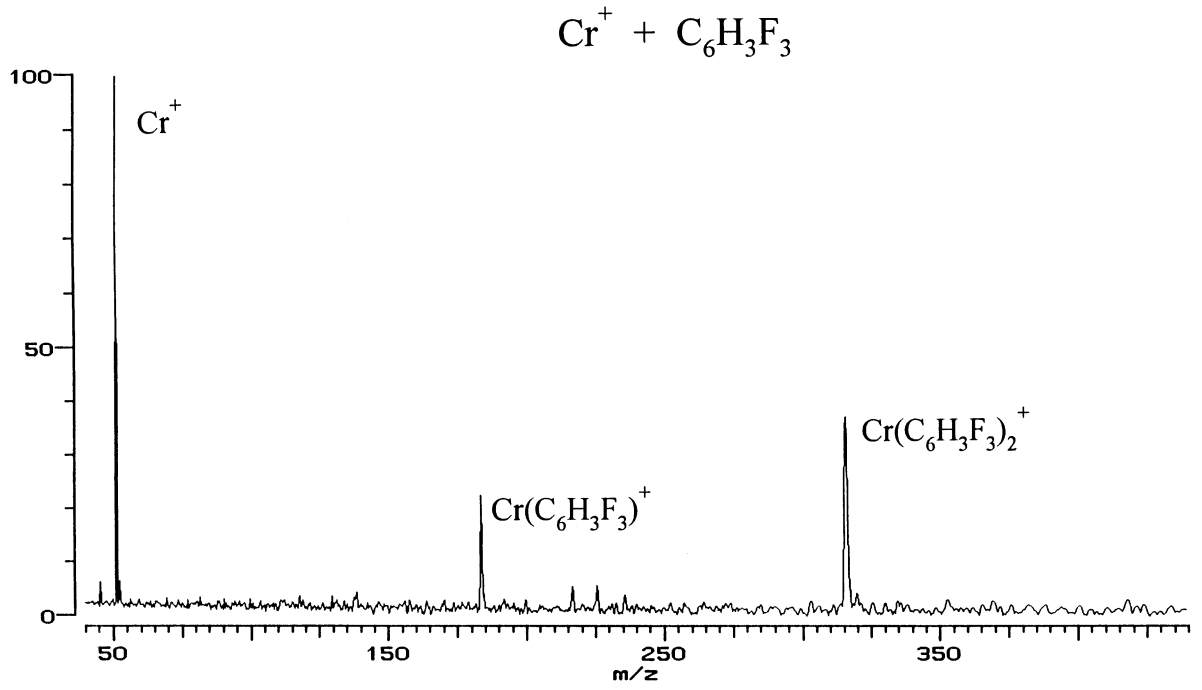

Fig. 2. Illustrative spectrum of Cr^+ reacting with 1,2,3-trifluorobenzene (9×10^{-8} Torr) at 25 s reaction time.

conditions (neutral pressure 9×10^{-8} Torr, reaction time 25 s) about a half of the Cr^+ ions ($m/z = 52$) have reacted to give the products CrL^+ ($m/z = 184$) and CrL_2^+ ($m/z = 316$).

An illustrative time plot for an association reaction of Cr^+ with fluorobenzene is given in Fig. 3. The radiative association rate constant can be extracted immediately from such a plot by fitting pseudo-first order kinetics to the decay of Cr^+ ions. Table 2 summarizes the experimental results.

Radiative association rates and efficiencies decrease strongly from fluorobenzene (efficiency 2.2%) to hexafluorobenzene (efficiency 0.014%), as can be seen from Table 2. For the cases where isomers exist, there are no dramatic differences between efficiencies for different isomers having the same number of fluorines.

4.2. Kinetic modeling

The process of deriving binding energy values from these rate constants must begin with an assessment of which sites exist, and which one is favored, for attachment of the metal ion. Our initial assumption that these would all be straightforward π complexes was seriously put in doubt by early results of the calculations, showing that whenever the neutral had two adjacent fluorine substituents, a favorable in-plane binding site bridging the adjacent fluorines was available having a calculated binding energy larger than the π-facial site. Table 3 summarizes the calculated energies of these two types of sites. Calculations also showed the possibility of binding of the metal ion to a single fluorine atom, but such nonbridging sites were always at least several kcal mol^{-1} less stable than the favored binding site; these single-F sites were not considered to play an important role in the binding, and are not described here, although for completeness they were included in the modeling procedure outlined below. (Fuller details of the various sites and their geometries and binding energies will be included in the companion paper [5].)

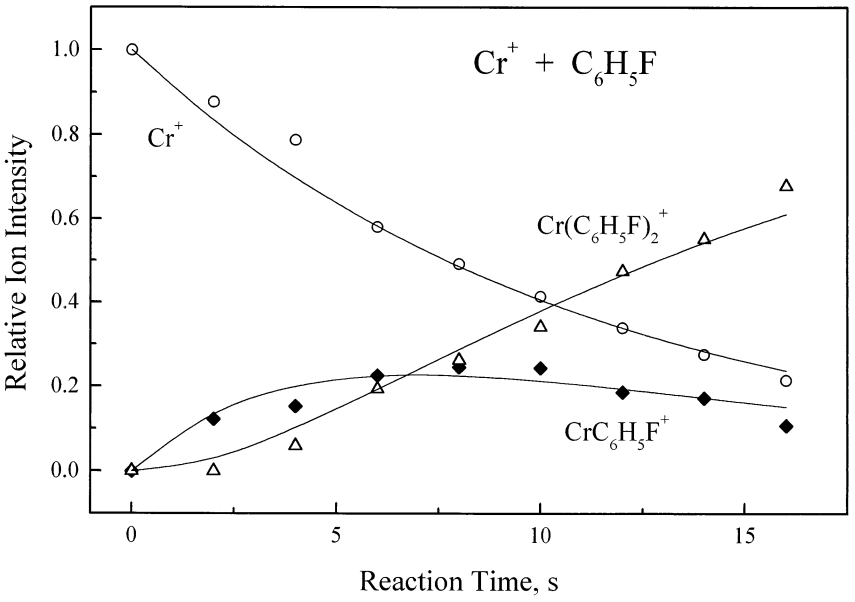

Fig. 3. Illustrative time plot for association of Cr^+ with fluorobenzene at 1.1×10^{-8} Torr. Lines represent the fit to simple sequential binding kinetics.

Table 2
Association kinetics results, and the "experimental" binding energies for the lowest-energy binding site derived by VTST-based modeling of the kinetics

Neutral	k_{ra}[a]	Φ, %[b]	E_b (kcal mol^{-1}) (RA kinetics modeling)
Benzene	0.23	1.7	44.5[c]
Fluorobenzene	0.40	2.2	39.1[c]
1,2-Difluorobenzene	0.17	0.66	32.9
1,3-Difluorobenzene	0.15	0.83	32.0[c]
1,4-Difluorobenzene	0.11	0.90	29.0[c]
1,2,3-Trifluorobenzene	0.070	0.26	29.3
1,2,4-Trifluorobenzene	0.038	0.22	29.9
1,3,5-Trifluorobenzene	0.027	0.23	26.3[c]
1,2,3,4-Tetrafluorobenzene	0.018	0.077	25.4
1,2,3,5-Tetrafluorobenzene	0.012	0.072	24.6
1,2,4,5-Tetrafluorobenzene	0.016	0.13	26.6
Pentafluorobenzene	0.0050	0.031	23.6
Hexafluorobenzene	0.0016	0.014	19.0

[a] Rate constants in units of 10^{-10} cm^3 mol^{-1} s^{-1}.
[b] Association efficiency, calculated as percent of ion-neutral collisions resulting in stabilized complexes.
[c] For these molecules, the lowest-energy binding site is calculated to be the π binding ring site. Otherwise Cr^+ binds most strongly at the bridging F–F binding site.

The site of binding is significant in the modeling because there are modest but not negligible differences in the geometries and IR radiative characteristics of different complex isomers. Differences of the order of 2 kcal mol^{-1} are found in the binding energies derived by radiative association kinetics modeling, depending on which site is assumed as the attachment site. In most cases one site is clearly more favorable than any others, and analysis assuming attachment at only this most favorable site was a satisfactory approximation. For those few cases in the present work where the two sites were calculated to be comparably favorable, a fully correct analysis should take into account the presence of complexes bound at both sites. It is not straightforward to make such an analysis accurately, but good approximate corrections can be applied to account for multiple sites. The modeled results shown in the "all sites" column of Table 3 give our best modeled binding energies based on inclusion of all binding sites in the analysis. We do not consider that the error in binding energy modeling because of the complications of multiple binding sites amounts to more than about 1 kcal mol^{-1}.

Table 3
Binding energies (kcal/mol) of $Cr(C_6H_{6-n}F_n)^+$ ($n = 0$ to 6) complexes determined via quantum chemistry calculations and radiative association modeling of kinetic data

	B3LYP DFT results[a]		Modeling results		
Ligand	π face	F–F	π face	F–F	All sites
Benzene	**38.9**		44.5		44.5
Fluorobenzene	**34.0**		39.1		39.1
1,2-Difluorobenzene	30.2	**31.0**	33.0	36.6	32.9
1,3-Difluorobenzene	**29.6**		32.0		32.0
1,4-Difluorobenzene	**28.3**		29.0		29.0
1,2,3-Trifluorobenzene	26.3	**27.9**	28.4	30.9	29.3
1,2,4-Trifluorobenzene	25.7	**28.3**	28.4	31.2	29.9
1,3,5-Trifluorobenzene	**23.5**		26.6		26.3
1,2,3,4-Tetrafluorobenzene	22.9	**25.5**	25.5	26.4	25.4
1,2,3,5-Tetrafluorobenzene	20.1	**25.4**	···	24.6	24.6
1,2,4,5-Tetrafluorobenzene	18.7	**25.8**	23.7	26.9	26.6
Pentafluorobenzene	17.8	**23.1**	24.8	24.6	23.6
Hexafluorobenzene	10.1	**20.4**	19.2	19.4	19.0

[a] Bold face indicates the site with highest binding energy, which is used in constructing Fig. 4.

The end result of the kinetic modeling procedure is an assignment of the binding energy that fits the experimental data for each system. As an indication of the importance of the assumptions used in setting up the modeling, the last three columns of Table 3 show the outcome of three different modeling procedures: the "π face" column shows the binding energy that fits the data on the assumption that only the π-facial site exists; the F–F column shows the binding energy that fits the data on the assumption that only the bridged-fluorine binding site exists; while the "all sites" column shows the fitted binding energy for the most favorable binding site, corrected by taking into account the contributions to the density of states of the complex from all the known binding sites on each molecule. It is seen that the differences in these modeling approaches are quite modest. The all-sites binding energies are reproduced in Table 2, which represent our final assignment of the "experimental" Cr^+ binding energies to the lowest-energy binding site for each of this series of compounds.

4.3. Binding energies

A comparison of the binding energies from VTST-based modeling with the B3LYP DFT-calculated values is given in Fig. 4. The agreement is quite good: the largest deviations are of the order of 10%, and in most cases agree much better than this. Cr^+ binding decreases sharply with addition of fluorines to the ligand, changing from 44.5 kcal/mol for benzene to 19.0 kcal/mol for hexafluorobenzene.

For the molecules not possessing an adjacent pair of fluorines, the strong, monotonic decrease in binding energy as substitution increases from zero to three fluorines gives a strong confirmation of the idea that addition of fluorines decreases the π electron density over the benzene ring, which results in weakening of Cr^+–L bonds. Each added fluorine weakens the Cr^+/ring bond by $\sim$5 kcal mol^{-1}. For the remaining cases where a bridging 1,2-difluoro binding site exists, the results confirm the weakening of the π binding in a more indirect way. As can be seen from Table 3, the fluorine-bridging binding site is expected to compete with or dominate over the π binding site for all of these cases; confirmation of our quantitative understanding of the bonding is provided by the excellent agreement between the B3LYP DFT-predicted binding energies and the "experimental" binding energies derived from the kinetic modeling. The F-bridging binding sites also decrease in binding energy with increasing fluorination, although not as rapidly as the

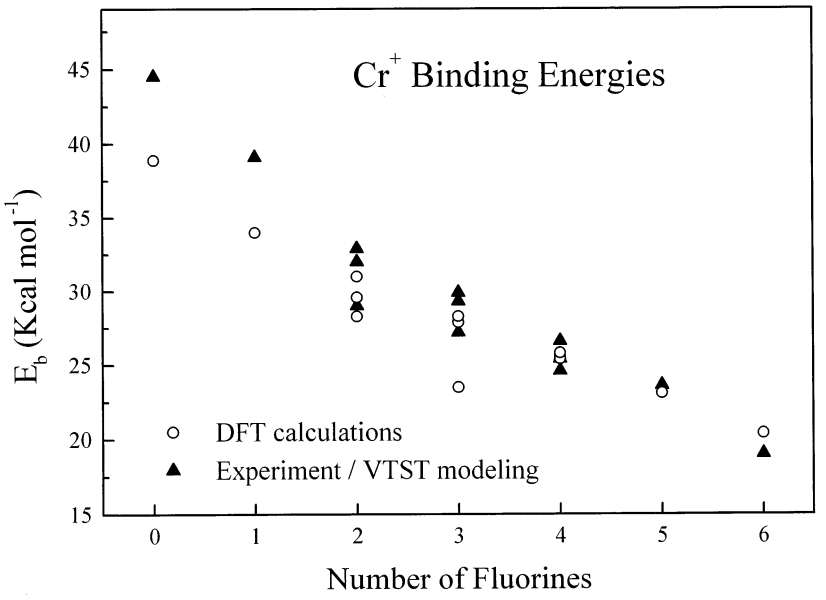

Fig. 4. Binding energies of Cr^+ with fluorobenzenes from VTST modeling of kinetic data (triangles) and from B3LYP DFT calculations (circles).

π sites. This can be attributed to increasing withdrawal of lone-pair electron density at the bridging site due to remote fluorine substituents.

The calculated energy difference between the structures of Cr^+/π-face bonding and Cr^+/bridged-fluorine bonding increases from 1,2-difluorobenzene (0.8 kcal mol^{-1}) to hexafluorobenzene (10 kcal mol^{-1}). As a matter of fact, the π binding site in hexafluorobenzene is the least favorable among all of the four binding sites that were identified for this complex.

4.4. Benzene and fluorobenzene

The association efficiency for benzene is a little smaller than for fluorobenzene (1.7% versus 2.2%) but still results in higher binding energy (44.5 kcal mol^{-1} versus 38.6 kcal mol^{-1}). This can be explained by the fact that the IR intensities are higher for the fluorobenzene complex, resulting in a higher photon emission rate k_r, and the frequencies are lower for the fluorobenzene complex, giving a higher density of states. Both of these effects lead to a smaller fitted binding energy. The smaller binding energy of fluorobenzene was further confirmed by competitive CID of the mixed complex $CrL_1L_2^+$, where L_1 is benzene and L_2 is fluorobenzene. This CID experiment (Fig. 5) resulted in exclusive loss of fluorobenzene ligand, confirming a higher binding energy for benzene.

5. Conclusions

VTST-based kinetic analysis of radiative association kinetics of chromium ions with the complete set of fluorobenzenes yielded the "experimental" binding energies for these systems. These "experimental" values are in good agreement with B3LYP DFT quantum-chemical calculations of the most favorable binding sites on the neutrals. The modeling is fairly insensitive to the assumption made about where the metal ion attaches to the ligand. It is also reasonably insensitive to the details of the modeling with respect to the simultaneous presence of multiple binding sites.

Chromium ion binding energy decreases as the number of fluorine atoms on the aromatic ring increases, by an amount of roughly 5 kcal mol^{-1}. In the cases for which a π-facial binding geometry is ex-

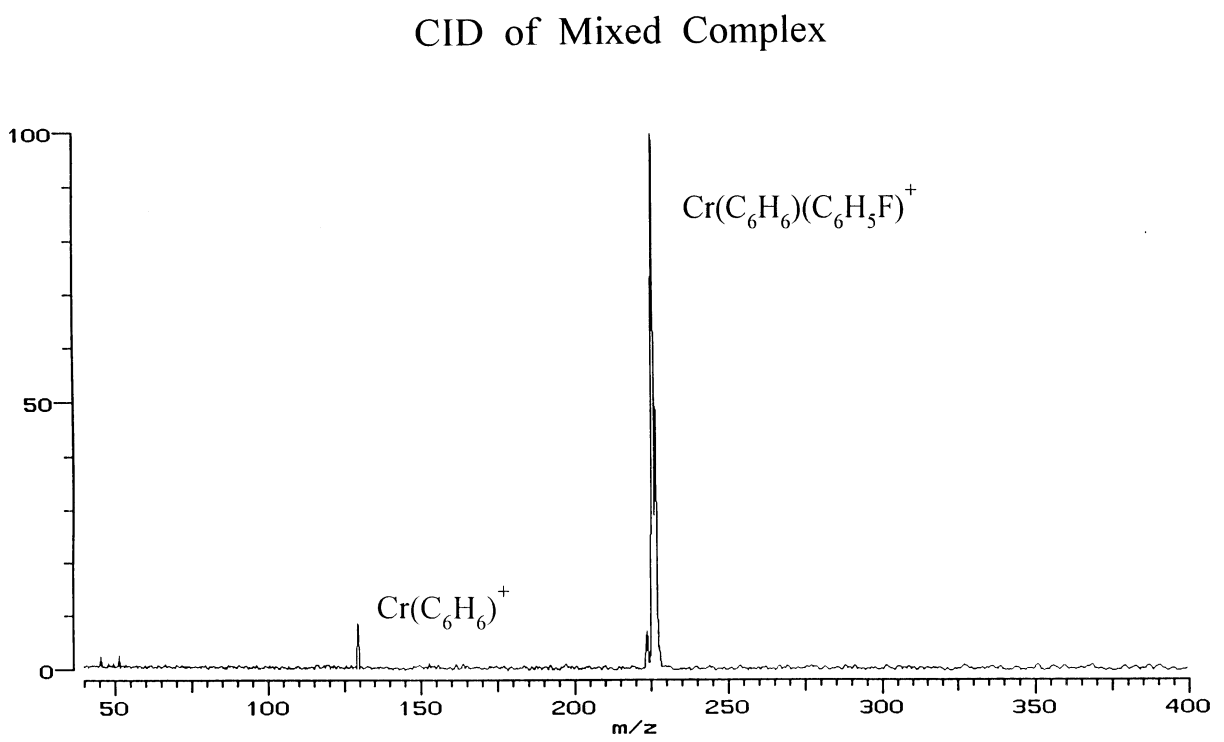

Fig. 5. Competitive CID of the Cr(benzene)(fluorobenzene)$^+$ complex, showing the predominant loss of the fluorobenzene ligand.

pected, this observation supports the picture that addition of each fluorine on the aromatic ring depletes π electron density above the ring and weakens Cr^+–L bonds. All of the molecules possessing two adjacent F substituents are predicted to favor an in-plane fluorine-bridging binding geometry, which is supported in an indirect way by the excellent agreement of these predictions with the "experimental" values. The binding also weakens with increasing numbers of fluorines in these bridged-fluorine complexes, which is attributed to withdrawal of lone-pair electron density by the presence of additional fluorines.

Acknowledgements

This work was supported in part by the National Science Foundation and by the donors of the Petroleum Research Fund, administered by the American Chemical Society.

References

[1] D. Schröder, H. Schwarz, J. Hrušák, P. Pyykkö, Inorg. Chem. 37 (1998) 624; D. Schröder, J. Hrušák, R.H. Hertwig, W. Koch, P. Schwerdtfeger, H. Schwarz, Organometallics 14 (1995) 312; J. Hrušák, R.H. Hertwig, D. Schröder, P. Schwerdtfeger, W. Koch, H. Schwarz, Organometallics 14 (1995) 1284.
[2] F. Meyer, F.A. Khan, P.B. Armentrout, J. Am. Chem. Soc. 117 (1995) 9740.
[3] C.-Y. Lin, R.C. Dunbar, Organometallics 16 (1997) 2691.
[4] B.C. Guo, J.W. Purnell, A.W. Castleman Jr., Chem. Phys. Lett. 168 (1990) 155.
[5] C.-N. Yang, V. Ryzhov, R.C. Dunbar, S.J. Klippenstein, manuscript in preparation.
[6] R.C. Dunbar, S.J. Klippenstein, J. Hrušák, D. Stöckigt, H. Schwarz, J. Am. Chem. Soc. 118 (1996) 5277.
[7] S.J. Klippenstein, Y.-C. Yang, V. Ryzhov, R.C. Dunbar, J. Chem. Phys. 104 (1996) 4502.
[8] C.-Y. Lin, Q. Chen, H. Chen, B.S. Freiser, Int. J. Mass Spectrom. Ion Processes 167/168 (1997) 713.
[9] C.W. Bauschlicher Jr., H. Partridge, Chem. Phys. Lett. 181 (1991) 129.
[10] I. Alkorta, J.J. Perez, H.O. Villar, J. Mol. Graphics 12 (1994) 3.

[11] D.A. Dougherty, Science 271 (1996) 163.
[12] J.C. Ma, D.A. Dougherty, Chem. Rev. 97 (1997) 1303.
[13] I. Alkorta, I. Rozas, J. Elguero, J. Org. Chem., 62 (1997) 4687.
[14] R.C. Dunbar, J. Phys. Chem. 102 (1998) 8946.
[15] Y.-P. Ho, R.C. Dunbar, Int. J. Mass Spectrom., in press.
[16] S.S. Xantheas, J. Chem. Phys. 104 (1996) 8821.
[17] GAUSSIAN 94, M.J. Frisch, G.W. Trucks, H.B. Schlegel, P.M.W. Gill, B.G. Johnson, M.A. Robb, J.R. Cheeseman, T. Keith, G.A. Petersson, J.A. Montgomery, K. Raghavachari, M.A. Al-Laham, V.G. Zakrzewski, J.V. Ortiz, J.B. Foresman, J. Cioslowski, B.B. Stefanov, A. Nanayakkara, M. Challacombe, C.Y. Peng, P.Y. Ayala, W. Chen, M.W. Wong, J.L. Andres, E.S. Replogle, R. Gomperts, R.L. Martin, D.J. Fox, J.S. Binkley, D.J. Defrees, J. Baker, J.P. Stewart, M. Head-Gordon, C. Gonzalez, J.A. Pople, Gaussian, Inc., Pittsburgh, PA, 1995.
[18] J.J. Fisher, T.B. McMahon, Int. J. Mass Spectrom. Ion Processes 100 (1990) 701.
[19] Y.-P. Ho, Y.-C. Yang, S.J. Klippenstein, R.C. Dunbar, J. Phys. Chem. 101 (1997) 3338.
[20] S.J. Klippenstein, R.C. Dunbar, Unpublished results.
[21] T. Su, W.J. Chesnavich, J. Chem. Phys. 76 (1982) 5183.
[22] S.J. Klippenstein, A.F. Wagner, R.C. Dunbar, D.M. Wardlaw, S.H. Robertson, E.W. Diau, VariFlex computer code, to be published.
[23] K.J. Miller, J.A. Savchik, J. Am. Chem. Soc. 101 (1979) 7206.
[24] R.C. Weast, Handbook of Chemistry and Physics, 54th ed., CRC, Cleveland, OH, 1973–1974.